Nanoscale

Cite this: *Nanoscale*, 2012, **4**, 5059

www.rsc.org/nanoscale

PAPER

Ultra-low power hydrogen sensing based on a palladium-coated nanomechanical beam resonator†

Jonas Henriksson, Luis Guillermo Villanueva‡* and Juergen Brugger

Received 16th March 2012, Accepted 20th May 2012
DOI: 10.1039/c2nr30639e

Hydrogen sensing is essential to ensure safety in near-future zero-emission fuel cell powered vehicles. Here, we present a novel hydrogen sensor based on the resonant frequency change of a nanoelectromechanical clamped–clamped beam. The beam is coated with a Pd layer, which expands in the presence of H_2, therefore generating a stress build-up that causes the frequency of the device to drop. The devices are able to detect H_2 concentrations below 0.5% within 1 s of the onset of the exposure using only a few hundreds of pW of power, matching the industry requirements for H_2 safety sensors. In addition, we investigate the strongly detrimental effect that relative humidity (RH) has on the Pd responsivity to H_2, showing that the response is almost nullified at about 70% RH. As a remedy for this intrinsic limitation, we applied a mild heating current through the beam, generating a few μW of power, whereby the responsivity of the sensors is fully restored and the chemo-mechanical process is accelerated, significantly decreasing response times. The sensors are fabricated using standard processes, facilitating their eventual mass-production.

Introduction

Hydrogen is a very promising candidate for replacing petrol as a pollutant-free energy carrier. However, when H_2 is mixed with air, it is flammable/explosive at concentrations between 4 and 75%.[1] To guarantee personal safety, sensitive, fast and cost-efficient H_2 sensors are needed.[2]

Palladium is one of the most used materials in hydrogen sensors because it features reversible absorption of hydrogen, leading to the formation of palladium hydride (PdH_x).[3] This material presents up to 80% higher resistivity and up to 3% larger lattice constant than pure Pd, and both processes are highly selective features of H_2 absorption. Sensors based on resistivity change have been the dominating type over the years,[4] but they present relatively slow response times and/or high power consumption, usually required to accelerate the response.[5] The use of nanoscale patterned, self-heating Pd-structures has recently allowed for significant improvements in both of those issues,[5–8] but with the number of sensors potentially needed, the power consumption has to be reduced even more.

Several works have also presented the chemo-mechanical effect of Pd expansion for H_2 sensing applications in different configurations, including Pd mesowires that close/open contacts under H_2,[9] bimorph cantilevers whose bending is monitored[10–12] or causes conduction in ordered arrays[13] and discontinuous films whose expansion causes percolation.[14,15]

Bimorph micro- and nano-mechanical structures are a convenient solution from the point of view of their compatibility with standard top-down techniques developed in the semiconductor industry over the years[16] and their ultra-low power consumption. However, deflection-based (or amplitude-based) mechanical sensors, regardless of the transduction technique, suffer from the fact that any external source of noise directly offsets the electrical signal that is the output from the device and thereby reduces the resolution of the sensor.

It is possible to circumvent this issue by using resonance-based mechanical sensors where the magnitude to be monitored is the natural frequency of the device. The mechanical resonant frequency of a structure is an extremely robust property towards external noise. Micro- and nano-electromechanical resonators are widely used in science and technology as sensors for mass spectrometry,[17] temperature,[18] gas concentration,[19] material deposition,[20] *etc.* They excel in providing a stable and precise resonant frequency, with very little susceptibility to external disturbances, such as vibrations or electronic noise.[21,22]

In this paper, we present the use of clamped-clamped mechanical resonators made out of a multi-layer stack of amorphous silicon (a-Si)/Cr/Au/Pd (750/5/30/30 nm) with a capacitive transduction scheme (Fig. 1) for the detection of hydrogen concentration.

As stated before, when Pd is exposed to hydrogen, the material transition to palladium hydride takes place, leading to expansion in the absence of external physical constraints. However, the boundary conditions of the fabricated clamped–clamped beams

Microsystems Laboratory, EPFL, Lausanne, Switzerland. E-mail: jonas.henriksson@epfl.ch; juergen.brugger@epfl.ch

† Electronic supplementary information (ESI) available. See DOI: 10.1039/c2nr30639e

‡ Current address: DTU Nanotech, Technical University of Denmark, Denmark. E-mail: lgv@lgvillanueva.info.

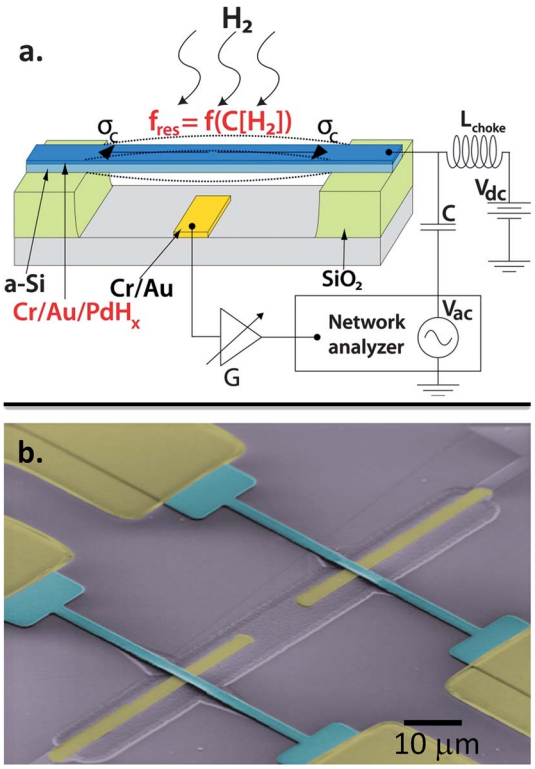

Fig. 1 (a) Illustration of actuation, readout and sensing principles. When H_2 is absorbed by the Pd, this causes an expansion in the material that creates a compressive stress in the beam, therefore shifting its resonant frequency. The frequency is detected using a two-port capacitive transduction technique. (b) Colored SEM image (purple = substrate, blue = beam, yellow = top and bottom electrodes) of a typical example of the fabricated structures. The suspended region is approximately 20 μm, with a width of 1.5 μm and a total thickness of 815 nm.

stop the film from expanding in the longitudinal direction of the beams, and a compressive stress is generated instead. This compressive stress effectively softens the beam and lowers its resonant frequency. The incorporation of hydrogen atoms into the Pd also increases the beam mass, therefore reducing its frequency. However, considering the atomic mass ratio between H and Pd, this latter effect is negligible compared to the former one (see ESI†). The relative change in resonant frequency of a mono-material beam can be expressed by the following expression for small stress loads (small relative change in the frequency):[23]

$$\Delta f/f_0 \approx -0.1475(\sigma/E)(L/t)^2 \quad (1)$$

where f_0 is the resonant frequency of the unstressed beam, σ is the longitudinal tensile stress in the beam, L and t are the length and thickness respectively, and E is the Young's modulus of the material. By using a multi-layered structure, the thickness ratio can be adapted in such a way that the sensor can cover a larger dynamic range.

This working principle type has already been explored in the past, delivering highly responsive temperature sensors[24,25] and even hydrogen sensors, with a minimum detectable concentration of hydrogen of 14 ppb[26] showing the great potential of nanomechanical resonators for H_2 sensing. Although being interesting for fundamental physical/chemical experiments, the system described there was operated in vacuum and made use of magnetomotive transduction. Both aspects lead to serious limitations for implementation as a hydrogen sensor for safety applications in the automotive industry – the former because of the problem of using a gas sensor that only functions in vacuum and the latter because of the need for very strong magnetic fields.

Here, we show the potential of a system operated at room temperature, atmospheric pressure and high relative humidity. We use capacitive transduction, which has great downscaling potential and the capability of monolithic integration with CMOS circuitry, critical for the final applicability of the system.[27] We show that our sensor has enough resolution to be used for safety regulation with power consumption of some hundreds of pW. In addition, we study the detrimental effects of relative humidity on the proposed sensing mechanism and show that highly localized heating extends the operable range into very humid environments without compromising ultra-low power operation.

Results

Response under dry conditions

The response of a typical sensor to the exposure of H_2 in dry N_2 can be seen in Fig. 2a, where the device is exposed to a 4% concentration of H_2 for 30 s followed by a flush in dry N_2 during 150 s. As shown, the resonant frequency shifts down as soon as H_2 enters the chamber, following an exponential law with a characteristic decay rate of around 30 s. After the first couple of exposures to H_2, during which a priming effect is observed, the frequency shift is highly reproducible (see ESI†). When the hydrogen line is closed and N_2 starts flowing into the chamber, the resonant frequency returns to its initial value, indicating that the structure has not been changed mechanically, neither by the diffusion, nor by the subsequent exodiffusion, of hydrogen into and out of Pd. This chemo-mechanical recovery also follows an exponential function, in this case with a decay rate of 45 ± 5 s (see ESI†).

Fig. 2b shows the response of a typical beam to different hydrogen concentrations, ranging from 0.5% up to 2.5%. The result shows an almost linear increase of response with concentration, illustrated in Fig. 2c. This linearity (within this concentration range) allows us to define a responsivity of the sensor, which depends on the time lapse (τ) after the onset of H_2, following eqn (2):

$$\Re(\tau) = \frac{\Delta f}{f_0}\Big/[\%\ H_2] = \Re(\infty)\left(1 - e^{-\frac{\tau}{T_{decay}}}\right) \approx (0.122 \pm 0.008)\left(1 - e^{-\frac{\tau}{29}}\right) \quad (2)$$

where the parameters have been extracted after non-linear fitting of the data in Fig. 2b. For the particular cases presented in Fig. 2c, $\Re(30\ s) \approx 0.078 \pm 0.001$ and $\Re(60\ s) \approx 0.107 \pm 0.002$ are the responsivities of the sensor per % of H_2 concentration after 30 and 60 s, respectively.

The general behavior of any fabricated beam is well outlined by eqn (2). A common decay time of $T_{decay} \approx 29 \pm 2$ s is determined. The only difference between individual beams is the response once the steady-state has been reached, which scales as L^2, as stated by eqn (1) for the range of concentrations shown in Fig. 2c. At hydrogen concentrations exceeding 3%, the response

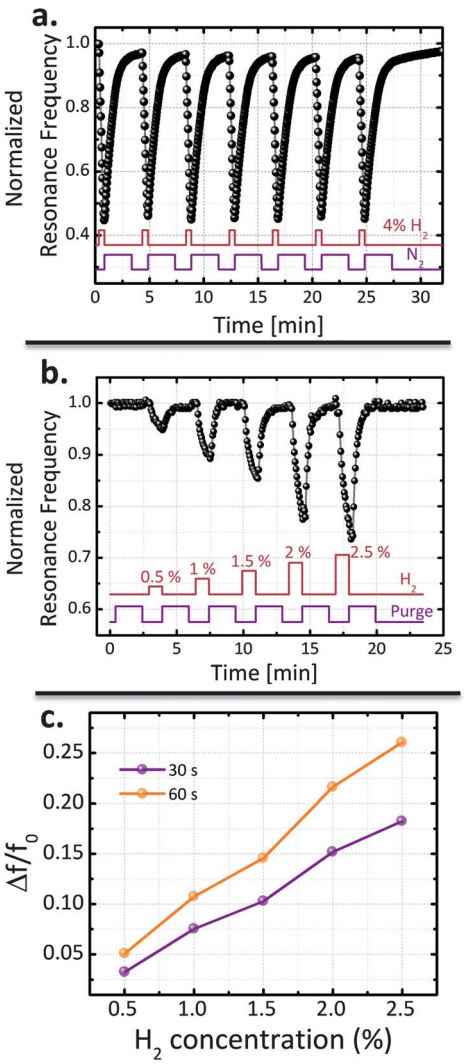

Fig. 2 *Sensor response under dry conditions.* (a) Relative response of a 6.5 MHz beam to flushes of 4% H_2 at 30 s intervals and subsequent 150 s purges with N_2. The reproducibility of the response is very high and no permanent changes in the beam are observed. (b) Relative response of a 1.3 MHz beam to a H_2 concentration increasing in steps from 0.5% to 2.5%, with each exposure lasting for 60 s. (c) Relative reduction of resonant frequency as a function of H_2 concentration of the device from (b) at 30 s and 60 s after the onset of H_2.

increases sharply by almost an order of magnitude, as can be seen by comparing Fig. 2a and b. Using eqn (1) while taking into account differences of length and initial stress, we estimate that the response observed in Fig. 2a supersedes the typical linear response, shown in Fig. 2b and c, by a factor of 9.

Effect of relative humidity

Our tests reveal two separate humidity-related effects: direct frequency shift caused by water adsorption (see ESI†) and a decrease in responsivity to H_2 (Fig. 3). The latter is of critical importance because, as can be seen in Fig. 3a, the response of the sensor gradually becomes weaker and weaker as RH increases until it reaches 70%, at which the sensor hardly shows any response. This is clearly shown in Fig. 3b, where the ratio

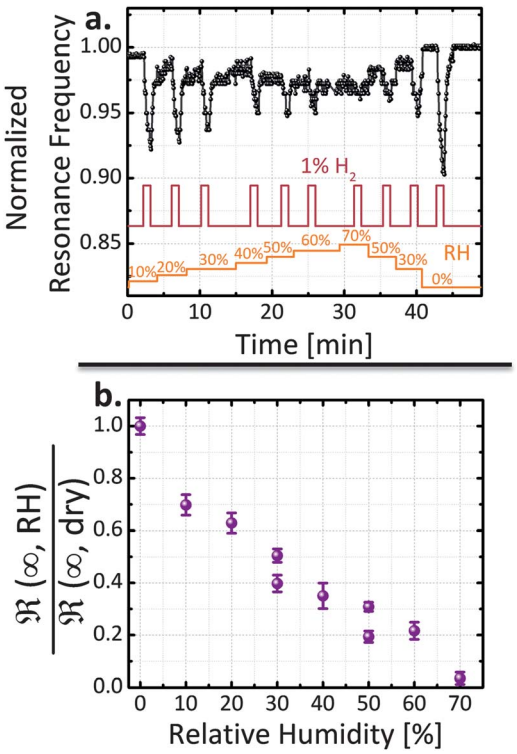

Fig. 3 *Sensor response and relative humidity.* (a) Response to 1% H_2 exposures lasting 60 s under different values of relative humidity. (b) Relative resonant frequency reduction, defined as the difference between the resonant frequency before and after the respective exposure, as a function of relative humidity.

between ℜ(60 s) at a given RH over ℜ(60 s) under dry conditions is plotted against RH. It can be seen how the responsivity at 30% RH is only half of the one measured under dry conditions and, at 70% RH, it is only about 2% of that.

In order to extend the sensor's workable regime into the full RH range, we apply local self-heating of the beam *via* Joule effect caused by a current flowing through the beam itself. The idea is to minimize water condensation on the beam by increasing its surface temperature.

Fig. 4 shows how the heating affects the beam responsivity to hydrogen. When RH is 50% and no current is applied, ℜ(60 s) is about 0.035. When a heating current of 2 mA is applied, ℜ(60 s) increases to about 0.077. When the heating current is increased to 3 mA, ℜ(60 s) increases to 0.092 showing almost a full recovery of the initial responsivity under dry conditions. A similar effect can be observed when the RH is elevated to 70% while keeping a current of 3 mA: ℜ(60 s) is about 0.082, only marginally lower than the one at 50% RH. Compared to the responsivity of an unheated beam at 70% RH shown in Fig. 3, it increases by a factor of almost 40. Rather than enhancing the response, the heating enables an effective countering of the deteriorative effect of humidity.

In addition to the effects just described, we observe an immediate drop in resonant frequency when a current is applied. This drop is mostly due to the compressive stresses generated by the thermal expansion of the beam materials. Using the material thermal expansion coefficients ($\alpha_{a\text{-}Si} = 2.6 \times 10^{-6}$, $\alpha_{Pd} = 11.8 \times 10^{-6}$, $\alpha_{Au} = 14.2 \times 10^{-6}$) in combination with eqn (1) to calculate

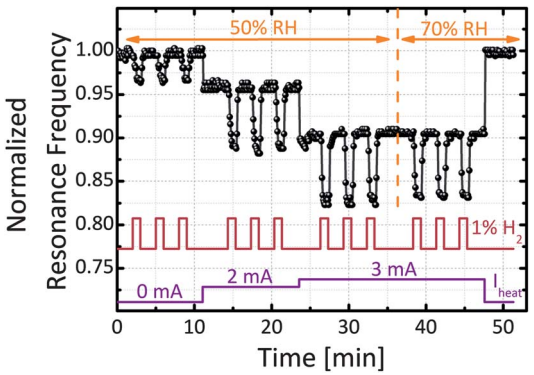

Fig. 4 Behavior improvement through self-heating. Response to H_2 under very humid conditions with and without a heating current. Four series of 3 × 60 s exposures to 1% H_2 were carried out with different RH and I_{heat} parameters.

the temperature corresponding to this drop in resonant frequency, we can estimate the temperature change to be $\Delta T \approx 6$ K for $I = 3$ mA, which is comparable to the results obtained *via* finite element simulations (see ESI†).

Discussion

The sensor response is highly reproducible, as illustrated by Fig. 2a. A priming effect can be seen only during the first couple of exposures (see Fig. S1 of the ESI†). This effect has been reported in the past for other Pd-based H_2 sensors[9,10,15] and we believe that in our case it is mainly caused by the presence of a few atomic layers of palladium oxide on the Pd–air interface, reducing the hydrogen absorption and applying some tensile stress on the beam.[10] When exposed to hydrogen, the oxide is removed by reduction to Pd. Although precise measurements of the oxidation time have not been performed, it has been seen that it is in the order of several days. This might impose some limitations for the eventual applicability of these sensors, but the issue could be bypassed by performing periodic maintenance or by priming the sensor every time it is switched on.

Three of the parameters that define the applicability of the sensor, *i.e.* responsivity, minimum detectable H_2 concentration and response time, are co-dependent. The latter parameter, response time, is usually defined as the time lapse at which 90% of the steady-state response has been reached since the onset of H_2. In our case this time is relatively long (more than 60 s), but this does not imply that the presented sensor is bound to respond slower than that. First, it is necessary to consider that the experimental setup is not optimized to characterize response times properly. In addition, our sensors respond with no appreciable delay to H_2 (the delay is smaller than the precision of our current setup – 1 s). This opens the possibility of operating the sensor "dynamically", *i.e.* without waiting until the steady state has been reached. At this point, it must be noted that the system does not reach its stationary state in any of the cases presented in Fig. 2, but still the response is clear. The responsivity of the sensor, given by eqn (2), depends on the mentioned time elapsed since H_2 onset and, if we consider the frequency noise of the sensor (measured to be $\sqrt{(\Delta f/f_0)^2} \lesssim 0.0025$, see ESI†), we obtain that the presented sensor could detect a 1% concentration of H_2 approximately within 0.6 s of the onset of exposure, which is within the typical requirements for a H_2 safety sensor.[2] In other words, it is possible to perform detection almost two orders of magnitude faster than the characteristic decay rate of the transient response of about 29 s. This also explains the co-dependence of responsivity, minimum detectable H_2 concentration and response time that we mentioned before. Once the detection time is fixed (*e.g.*: $\tau = 1$ s) the responsivity can be estimated using eqn (2) (*e.g.* $\Re(1\text{ s}) \approx 0.0041 \pm 0.0003$) as well as the minimum detectable concentration ($[H_2] \approx 0.6\%$). In addition, it is possible to estimate the ultimate detection limit of these sensors if we assume that enough time is allowed so that they reach their steady-state. In that case $\Re(\infty) \approx 0.122 \pm 0.008$ and the minimum detectable concentration is $[H_2] \approx 0.02\%$. These ultimate limits are determined by the dimensions of the particular beam used according to eqn (1) and the frequency stability. The latter is generally a parameter that needs to be estimated for each particular device. We believe that the major limitation to this parameter in our case originates from the noise introduced in the transduction scheme. This noise will diminish if an on-chip amplifying circuitry is used.[27]

Fig. 2c shows the linearity of the response of these sensors up to 2.5% of H_2 concentration and while the produced frequency shift is relatively small. If the shift is bigger, the response should follow a square root law with the load (see ESI†). In addition, as shown, the response increases sharply when the H_2 concentration is higher than 3%. We believe this corresponds to a well-known phenomenon in Pd: the α-phase to β-phase transition.[3] When this transition occurs (generally reported to happen between 1 and 3%), the material shows a switch-like behavior, leading to a very large increase of the H/Pd ratio per added unit of H_2 partial pressure, which causes a large increase in material expansion. We observe a response increase of approximately one order of magnitude in a narrow concentration interval of around 3–4%, which is in agreement with previous works.[11] The fact that the transition happens at a higher concentration than originally reported for the system[3] might be due to the adhesion layer we use, which has been reported as a way of suppressing the phase transition for lower concentrations.[28] In order to linearize the response and push the threshold for the phase transition even higher, it is possible to use active layers of Pd-alloys (*e.g.* with Ag[11] or Ni[29]) instead of pure Pd. However, this solution comes with a trade-off because the responsivity decreases and the fabrication is more challenging due to the issues that working with alloys entails.

The chemo-mechanical process that causes the frequency drop has, as discussed above, a characteristic decay time of 29 ± 2 s. This is true for the different tested beams regardless of the concentration of hydrogen. As noted for Pd nanowires,[5] the process is not limited by the diffusion of hydrogen into Pd, but rather by its adsorption on the surface. Recovery also follows an exponential decay, but in this case the characteristic time is different if the concentration is below 3% (about 15 ± 3 s) or above 3% (about 45 ± 5 s). This fact is not coherent with previously reported sensors that always showed slower dynamics in the recovery,[5] and we believe that this is related to the fact that air (not N_2) was used for flushing in all the below 3% experiments. Even though we have already stated that it is not necessary to accelerate these dynamics to improve the applicability of the presented sensors, two known solutions could reduce the

response and recovery times: making the Pd layer porous and/or nanopatterned[30] or increasing the temperature of the layer,[31] as we discuss below.

Relative humidity poses a serious problem for the proposed detection scheme. As shown in Fig. 3, the responsivity drops almost linearly with RH and at around 70% RH there is hardly any response anymore. The reasons for this are not clear but we think that water condensation on top of the active Pd layer either arrests its catalytic activity or stops hydrogen from diffusing into the metal and therefore nullifies the chemo-mechanical reaction that provides the sensing response. To increase the range of operability of the sensor, a specialized packaging can be used, so that the RH level in the surroundings of the sensor is kept constant. As an alternative, we propose here the use of a mild local heating of the device.

As can be seen in Fig. 4, the responsivity is greatly enhanced when a small current is passed through the beam, therefore slightly increasing its temperature ($\Delta T < 6$ K). This heating is insufficient to cause ignition of a H_2–O_2 mixture and, as it is highly localized, the required power is relatively low. Heating has been used over the years on Pd-based H_2 sensors[5,31] in order to improve sensitivity and/or response time. However, in those cases, the power consumption is generally much higher than in our systems.

The observed enhancement of the responsivity (for high values of RH) by heating is partially derived from a reduction of the water condensation on the beam surface, as the air capacity to sustain H_2O vapor increases with temperature. In other words, to have the same amount of water condensed on the beam it would be necessary to have a higher RH when the beam is being heated. We can, therefore, define an *effective* RH that corrects for the effect of this heating.[32] For example, the water condensation on the beam at 20 °C, surrounded by an environment at 20 °C and 50% RH, is equivalent to condensation on the beam at 25 °C in an environment at 20 °C and 70% RH. When comparing the results of the unheated beam at 50% RH and heated beam at 70% RH, we can see that the responsivity of the latter is about twice the responsivity of the former. The origin of this extra effect can be an underestimation of the effect of temperature, an underestimation of the temperature itself or an enhancement of the chemo-mechanical process which we have not considered in our model.

In addition, after careful fitting of each of the responses it is possible to see how the system responds when heated by a 3 mA current, following an exponential function with a decay rate of around 5 s, which is almost 6 times faster than the response time of the unheated beam. This is consistent with previous reports on Pd sensors that use heating to precisely improve their response time.[5,31] It is not the purpose of this paper to analyze the dependence between the response time and the temperature in detail, but in the ESI† an Arrhenius plot of the response times is shown, yielding an approximately linear response with activation energy of the same order of the ones reported in the literature.[5]

Conclusions

We have presented here a mechanical resonant sensor for hydrogen detection. The detection is based on the frequency shift of the beam induced by the stress generated in Pd when hydrogen is absorbed. The devices are fabricated using standard micro-fabrication techniques, demonstrating the feasibility for mass-production. The electrostatic transduction implies extremely low power consumption, in the order of hundreds of pW.

The response is highly reproducible, with no determinable delay between the onset of hydrogen and the beginning of the response. As the saturation time of H diffusing into a Pd thin film measures in the range of 100 μs to 1 ms and the time needed for dissociation and recombination is even shorter, both response and recovery times are limited by hydrogen adsorption and desorption respectively. Neither of them is observed to be affected by RH, but we show that they can be shortened by a factor of 6 by applying mild local heating, $\Delta T < 6$ K, to the beam.

The response of the sensors is linear up to a hydrogen concentration of 2.5%. Beyond that, a material phase transition causes a sharp increase in the response. In any case, the responsivity can be defined as a function of the elapsed time since the onset of hydrogen and the sensor can be used in dynamic mode, without waiting to reach the steady state, so that the detection can be performed faster. Our results indicate a minimum detectable concentration of 0.6%, 1 s after the onset of hydrogen. This value can be further reduced through the monolithic integration of an amplifying circuitry.

We also report that humidity decreases the responsivity and almost annihilates it completely at 70% RH. By passing a mild heating current through the beam causing around 5 K of temperature increase, this problem is solved and the responsivity is almost the same as the one obtained under dry conditions. This can be explained by a reduction in the H_2O condensation onto the beam surface. The heating also introduces thermal dilatation, causing compressive stress, which lowers the resonant frequency of the beam.

In conclusion, the Pd based H_2 sensing beam resonator represents a highly versatile, robust and scalable technology with very attractive features such as precise readout, large dynamic range, no necessity for heating under normal conditions and the ability to work at very high RH levels.

Methods

Fabrication

A silica substrate is used for high electric isolation. The electrodes (Cr/Au) are deposited by PVD and patterned onto the substrate by lift-off. A sacrificial layer of SiO_2 is sputtered onto the substrate, followed by a layer of amorphous Si. The beam metal layer (Cr/Au/Pd/Ti) is deposited by PVD and patterned through lift-off. The metal layer is used as mask during a dry Si etching process. The Ti protection layer is stripped in a weak HF bath. Hence, the top electrodes (Cr + Au) are deposited by PVD and patterned by lift-off. A resist mask is patterned in order to determine which part of the structure is to be released. The etching of the sacrificial SiO_2 is done in a bath containing NH_4F. The resist is then stripped in O_2 plasma and the process is finished. All fabrication steps are made in full-wafer scale in order to guarantee cost-efficiency.

Electrical detection

The beam resonant frequency is measured by monitoring the transmitted power induced by the actuation. This two-port technique is illustrated in Fig. 1a. We send AC power from

a network analyzer to one port of the device (*e.g.* top electrode) passing through a bias-tee (Mini-Circuits, ZFBT-4R2GW+) that adds a DC component to the AC signal. The other port (*e.g.* the bottom electrode) is connected to an amplifier which passes on the signal as input to the network analyser. The particular parameter values were optimized for each beam but the voltage ranges were $V_{DC} = 20$–30 V and $V_{AC} \approx 5$–10 dBm. The motional resistance of our devices was of the order of several GΩ, which yields a power consumption of a few hundreds of pW.

H_2 exposure

During the exposure tests, the device is positioned inside a gas chamber. Before exposure, the chamber is flushed with air/N_2. When mixing is needed to have the desired gas concentration, the mixing of different gases is stabilized by flushing to an external exhaust before opening the valve to the test chamber. The flow rate is kept at 1000 ml min^{-1}, independent of H_2 concentration for convenience. In a separate experiment, the resonant frequency was proven independent of the flow rate.

Acknowledgements

This work has been partially financed through the European Coordination Action NanoICT. The authors thank C. Beluche and Microchemical Systems SA for assistance in some of the H_2 exposure experiments, J. Arcamone for useful comments on the transduction technique, and F. Favier for useful comments on H_2 sensing. We thank the CMI-EPFL staff for their valuable help with the fabrication. L. G. V. thanks the European Commission for its financial support through the Marie Curie Program (PIOF-GA-2008-220682).

Notes and references

1 P. Soundarrajan and F. Schweighardt, *Hydrogen Sensing and Detection*, CRC Press, Taylor & Francis Group, 2009.
2 B. Knight and T. Clark, http://www.lanl.gov/orgs/mpa/mpa11/FinalReportforDOESensorsContractUTRC.pdf, 2005.
3 F. A. Lewis, *The Palladium Hydrogen System*, Academic Press, London, 1967.
4 T. Hubert, L. Boon-Brett, G. Black and U. Banach, *Sens. Actuators, B*, 2011, **157**, 329–352.
5 R. M. Penner, F. Yang and D. K. Taggart, *Small*, 2010, **6**, 1422–1429.
6 R. M. Penner, F. Yang and D. K. Taggart, *Nano Lett.*, 2009, **9**, 2177–2182.
7 P. Offermans, H. D. Tong, C. J. M. van Rijn, P. Merken, S. H. Brongersma and M. Crego-Calama, *Appl. Phys. Lett.*, 2009, **94**, 223110.
8 M. H. Yun, Y. Im, C. Lee, R. P. Vasquez, M. A. Bangar, N. V. Myung, E. J. Menke and R. M. Penner, *Small*, 2006, **2**, 356–358.
9 R. M. Penner, F. Favier, E. C. Walter, M. P. Zach and T. Benter, *Science*, 2001, **293**, 2227–2231.
10 D. R. Baselt, B. Fruhberger, E. Klaassen, S. Cemalovic, C. L. Britton, S. V. Patel, T. E. Mlsna, D. McCorkle and B. Warmack, *Sens. Actuators, B*, 2003, **88**, 120–131.
11 S. Okuyama, Y. Mitobe, K. Okuyama and K. Matsushita, *Jpn. J. Appl. Phys.*, 2000, **39**, 3584–3590.
12 Z. Hu, T. Thundat and R. J. Warmack, *J. Appl. Phys.*, 2001, **90**, 427.
13 T. Kiefer, A. Salette, L. G. Villanueva and J. Brugger, *J. Micromech. Microeng.*, 2010, **20**, 105019.
14 T. Xu, M. P. Zach, Z. L. Xiao, D. Rosenmann, U. Welp, W. K. Kwok and G. W. Crabtree, *Appl. Phys. Lett.*, 2005, **86**, 203104.
15 T. Kiefer, L. G. Villanueva, F. Fargier, F. Favier and J. Brugger, *Appl. Phys. Lett.*, 2010, **97**, 121911.
16 M. J. Madou, *Fundamentals of Microfabrication*, CRC Press, Boca Raton, FL, 1997.
17 A. K. Naik, M. S. Hanay, W. K. Hiebert, X. L. Feng and M. L. Roukes, *Nat. Nanotechnol.*, 2009, **4**, 445–450.
18 C. M. Lin, T. T. Yen, V. V. Felmetsger, M. A. Hopcroft, J. H. Kuypers and A. P. Pisano, *Appl. Phys. Lett.*, 2010, **97**, 083501.
19 M. Li, E. B. Myers, H. X. Tang, S. J. Aldridge, H. C. McCaig, J. J. Whiting, R. J. Simonson, N. S. Lewis and M. L. Roukes, *Nano Lett.*, 2010, **10**, 3899–3903.
20 J. Arcamone, M. Sansa, J. Verd, A. Uranga, G. Abadal, N. Barniol, M. van den Boogaart, J. Brugger and F. Perez-Murano, *Small*, 2009, **5**, 176–180.
21 C. J. Zuo, N. Sinha, J. Van der Spiegel and G. Piazza, *J. Microelectromech. Syst.*, 2010, **19**, 570–580.
22 L. G. Villanueva, R. B. Karabalin, M. H. Matheny, E. Kenig, M. C. Cross and M. L. Roukes, *Nano Lett.*, 2011, **11**, 5054–5059.
23 R. B. Karabalin, L. G. Villanueva, M. H. Matheny, J. Sader and M. L. Roukes, *Phys. Rev. Lett.*, 2012, **108**, 236101.
24 T. Larsen, S. Schmid, L. Grönberg, A. O. Niskanen, J. Hassel, S. Dohn and A. Boisen, *Appl. Phys. Lett.*, 2011, **98**, 121901.
25 A. K. Pandey, O. Gottlieb, O. Shtempluck and E. Buks, *Appl. Phys. Lett.*, 2010, **96**, 203105.
26 X. M. H. Huang, M. Manolidis, S. C. Jun and J. Hone, *Appl. Phys. Lett.*, 2005, **86**, 143104.
27 J. Arcamone, M. A. F. van den Boogaart, F. Serra-Graells, J. Fraxedas, J. Brugger and F. Perez-Murano, *Nanotechnology*, 2008, **19**, 305302.
28 K. R. Kim, J. S. Noh, J. M. Lee, Y. J. Kim and W. Lee, *J. Mater. Sci.*, 2010, **46**, 1597–1601.
29 R. C. Hughes and W. K. Schubert, *J. Appl. Phys.*, 1991, **71**, 542.
30 J. F. Patton, S. R. Hunter, M. J. Sepaniak, P. G. Daskos and D. B. Smith, *Sens. Actuators, A*, 2010, **163**, 464–470.
31 W. C. Liu, H. J. Pan, H. I. Chen, K. W. Lin, S. Y. Cheng and K. H. Yu, *IEEE Trans. Electron Devices*, 2001, **48**, 1938–1944.
32 A. L. Buck, *J. Appl. Meteorol.*, 1981, **20**, 1527–1532.

